View metadata, citation and similar papers at core.ac.uk
brought to you by CORE
provided by UCL Discovery

PROCEEDINGS OF SPIE

SPIEDigitalLibrary.org/conference-proceedings-of-spie

Integrating III-V quantum dot lasers on silicon substrates for silicon photonics

M. Liao
S. Chen
M. Tang
J. Wu
W. Li
K. Kennedy
I. Ross
A. Seeds
H. Liu

SPIE.

Downloaded From: https://www.spiedigitallibrary.org/conference-proceedings-of-spie on 9/1/2017 Terms of Use: https://spiedigitallibrary.spie.org/ss/TermsOfUse.aspx

Invited Paper

Integrating III-V quantum dot lasers on silicon substrates for silicon photonics

M. Liao[a], S. Chen[a], M. Tang[a], J. Wu[a], W. Li[b], K. Kennedy[b], I. Ross[b], A. Seeds[a], H. Liu[a]

[a]Department of Electronic and Electrical Engineering, University College London, London WC1E 7JE, UK
[b]Department of Electronic and Electrical Engineering, University of Sheffield, Sheffield S1 3JD, UK

ABSTRACT

The realization of efficient III-V lasers directly grown on Si substrates is highly desirable for large-scale and low-cost silicon based optoelectronic integrated circuits. However, it has been hindered by the high threading dislocation (TD) density generated at the interface between III-V compounds and Si substrates. Introducing dislocation filter layers (DFLs) to suppress the TD propagation into the active region becomes a key factor for realising lasers with advanced performance. In this paper, optimization of InGaAs/GaAs DFLs in III-V quantum dot (QD) lasers on Si is demonstrated. Based on these optimized DFLs and other strategies, we have achieved a high performance electrically pumped QD laser on a Si substrate with threshold current density of 62.5 A cm^{-2}, over 105 mW output power, maximum operation temperature of 120 °C and over 100,158 h of extrapolated lifetime.

Keywords: Molecular beam epitaxy, quantum dots, lasers, silicon photonics

1. INTRODUCTION

According to the Moore's law, the number of transistors per square inch on integrated circuit (IC) doubles every 18 months [1], increasing processing speed. However, the shortcomings of metal interconnections increase as the speed increases, such as heat dissipation, current leakage and chemical or material issues. Substituting metal connections with optical connections is one of the promising ways around these limitations. Although Si photonics has been studied intensively and has borne fruit [1], a reliable and high-efficiency Si-based light-emitting source remains a research challenge due to the indirect bandgap structure of silicon which is not an efficient emitter material [2,3]. Comparing with Si, III-V compounds have superior electronic and optical properties as the active region for a light emitter. Thus, the integration of III-V compounds on Si substrates, by wafer bonding or monolithic growth, has been considered as the most practical approach to achieve a Si-based light emitter [5-12]. Despite the attractive results, with milliwatt output power and high temperature operation (over 100 °C) being achieved from lasers by using wafer bonding [13], this method still suffers from low yield for massive production. Monolithic growth of III-V compounds on Si substrates, provides an ideal solution for laser fabrication.

However, there are still some issues that limit the performance of lasers when using monolithic growth method. Firstly, due to the polar and non-polar epitaxial growth of III-V compounds and Si substrate, the formation of antiphase domains (APDs) between III-V/Si results. Moreover, lattice mismatch and incompatible thermal expansion coefficients between III-V compounds and Si material are the major issues of the monolithic growth method, which will introduce a high density of threading dislocations (TDs) [4]. The APDs can be eliminated by using off-cut Si substrates and multi-step growth method. However, a tougher task is to deal with the high density of TDs. These TDs may propagate to the active region and cause non-radiative recombination, which leads to the degradation of laser devices. Strained layer superlattice (SLS) structures, i.e., dislocation filter layers (DFLs), could play a crucial role to suppress the propagations of TDs into the active region. Although the density of TDs could be reduced significantly after introducing DFLs, an advanced InAs/GaAs dot-in-a-well (DWELL) structure is desirable as the active region. This is because the unique properties of quantum dots (QDs), including low defect sensitivity, low threshold current density and temperature insensitive operation,

Silicon Photonics XII, edited by Graham T. Reed, Andrew P. Knights, Proc. of SPIE Vol. 10108, 101081A
© 2017 SPIE · CCC code: 0277-786X/17/$18 · doi: 10.1117/12.2249761

Downloaded From: https://www.spiedigitallibrary.org/conference-proceedings-of-spie on 9/1/2017 Terms of Use: https://spiedigitallibrary.spie.org/ss/TermsOfUse.aspx

which can lead to more stable and better performance of QD lasers compared with quantum well (QW) structure laser [14-16].

In this work, we first optimized the InGaAs/GaAs SLSs DFLs by adjusting growth conditions of GaAs spacer layer and structures of SLSs [17]. After that, based on this optimization of DFLs, we also combine the strategies of a nucleation layer made of AlAs and in-situ thermal annealing of DFLs to achieve a low dislocation density of 1×10^5 cm^{-2} in the III-V epilayers. These methods contribute to a high performance III-V QD on Si laser with a low threshold current of 62.5 A cm^{-2} and over 105 mW output power at room temperature under continuous-wave (c.w.) operation. Finally, a lifetime study is implemented on this Si-based InAs/GaAs QD. Over 100,158 hours extrapolated lifetime suggest a high feasibility of delivering commercial III-V QD lasers directly grown on Si substrates [18].

2. OPTIMIZATION OF DFLS OF INAS/GAAS QD LASERS ON SI

2.1 Epitaxial Growth structure

In order to optimize the DFLs, a typical QD laser structure was grown on Si substrate by solid-source molecular beam epitaxy (MBE) as shown in Figure 1. A phosphorous-doped Si(100) wafer with a 4° offcut to the [011] plane was used as the substrate. The Si substrate was first prepared by oxide desorption at 900 °C for 30 min, and then a 1 µm GaAs buffer layer was grown with two steps: first 30 nm growth of GaAa layer at 380 °C with 0.1 monolayers/s (ML/s) growth rate and the remaining 970 nm GaAs was grown at high temperature with 0.7 ML/s growth rate. Three layers of InGaAs/GaAs SLSs for DFLs were utilized, each set of DFL including a 350 nm GaAs spacer layer and InGaAs/GaAs SLSs. In this DFL optimization, the first study is to investigate the growth condition of SLSs and GaAs spacer layer. Two different growth methods are introduced as illustrated in Fig. 2(a): in method I, a 350 nm GaAs spacer layer was grown with the temperature heating up from 420 °C to 610 °C, while in method II, the GaAs layer was grown at a stable temperature of 610 °C. In both cases, InGaAs/GaAs SLSs were grown at 420 °C. In additional, we also studied the influence of indium composition and thickness of GaAs in In_xGa_{1-x}As/GaAs SLSs on the efficiency of DFLs by changing x=0.16, 0.18 and 0.2 for indium composition and the GaAs thickness to 8, 9 and 10 nm in SLSs. For the active region of the laser structure, five sets of InAs/GaAs DWELL structure were sandwiched between GaAs/AlGaAs layers. Each set of DWELL was assembled by 3 ML InAs QDs which were deposited on 2 nm InGaAs and cladded by 5 nm GaAs and 6 nm InGaAs. The DWELLs were grown at 510 °C while each layer was separated by a 45 nm spacer layer of GaAs. Figure 2 (b) shows the AFM image of InAs/GaAs QDs with 3.8×10^{10} cm^{-2} of dot density.

Figure 1. Schematic diagram of InAs/GaAs QD structures grown on a Si substrate.

Downloaded From: https://www.spiedigitallibrary.org/conference-proceedings-of-spie on 9/1/2017 Terms of Use: https://spiedigitallibrary.spie.org/ss/TermsOfUse.aspx

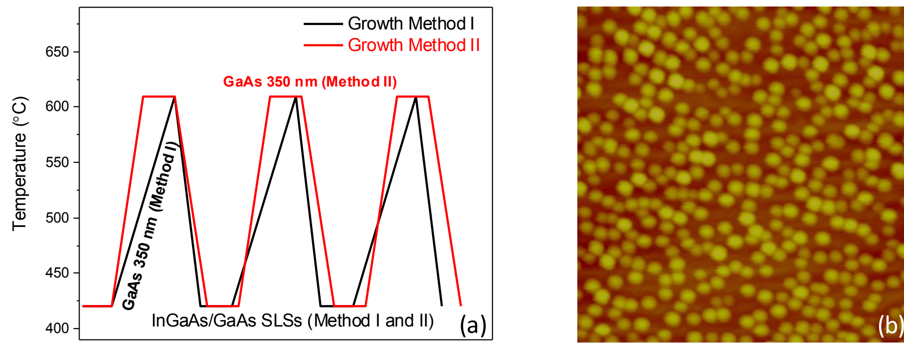

Figure 2. (a) The schematic of two growth method of DFLs. (b) AFM image of InAs/GaAs QDs.

2.2 Results and Discussion

To understand the effect of DFLs, photoluminescence (PL) peak intensity measurements are performed from sample A to F, which are shown in Table 1. These six samples are divided into three group studies: i) sample A and B used growth method I and II of spacer layers; ii) indium composition of $In_xGa_{1-x}As$ DFLs was changed to x=0.16, 0.18 and 0.2 in sample C, B and D, respectively; iii) studies of the thickness of GaAs in SLSs were undertaken in samples B, E and F, which the thickness varies from 10 nm to 8 nm. Fig. 3 gives the measurement results of PL peak intensity and full wave at half maximum (FWHM) of these three group studies at room temperature. When we used method II to grow GaAs spacer layer at temperature 610 °C, a three times stronger PL intensity was observed than that when the samples were grown by using method I (sample A), but the wavelength and FWHM keep almost unchanged as shown in Fig. 3(a). These PL emissions represent a significant improvement of DFLs using growth method II, and this advance can be attributed to the improved material quality after in-situ annealing of SLSs. Compared with growth method I, method II provides a high temperature growth condition for the GaAs spacer layer. This high temperature increases the motions of dislocations; this can lead them to meet and eliminate each other so that a low defect density was achieved on sample B. In this case, less non-radioactive recombination will occur in the active region, which could explain why a much higher PL peak intensity was achieved in growth method II.

In Fig.3 (b), the PL intensity spectra of samples B, C and D are presented with different indium composition of SLSs. When x= 0.18, we achieved the maximum PL intensity value from sample B, which is about 30 % and 40 % higher than that of sample C and D, respectively. Although the purpose of SLSs is to stop and annihilate dislocations, unfortunately a higher indium composition may cause an increase in strain-induced defects in DFLs instead of suppressing them. In contrast, a lower indium composition in InGaAs might lead to degrading the efficiency of DFLs in blocking the propagation of dislocations. In this study, a compromise of indium composition between the generation of strain-induced defects and the efficacy of SLSs was determined. It is a good balance of x=0.18, which provides the best crystal quantity.

Moreover, the effect of thickness of GaAs in SLSs on the performance of DFLs was investigated. As shown in Fig. 3(c), it is clear that the PL intensities of sample B and E have comparable values with 10 nm and 9 nm thickness of GaAs. However, the PL intensity of sample F, who has 8 nm thickness, is significant lower (50%) than sample B and E. This could be explained by the accumulated strain in too thin GaAs layers in SLSs which degrades the quality of DFLs. To figure out the working details of DFLs, cross-sectional transmission electron microscopy (TEM) images of DFLs in sample B is shown in Fig. 4. As we can see, the three sets of SLSs can stop and annihilate TDs effectively. According to these three group studies, the most effective DFLs were grown by in-situ thermal annealing method with x =0.18 and 10 nm thickness of GaAs in SLSs.

Downloaded From: https://www.spiedigitallibrary.org/conference-proceedings-of-spie on 9/1/2017 Terms of Use: https://spiedigitallibrary.spie.org/ss/TermsOfUse.aspx

Table 1. The PL peak intensity and FWHM of samples with different growth method, indium composition and GaAs thickness.

Sample	Growth type	x of $In_xGa_{1-x}As$	GaAs Thickness (nm)	PL peak intensity (a.u)	FWHM (nm)
A	I	0.18	10	1.2	40.5
B	II	0.18	10	4	40.3
C	II	0.16	10	2.6	39.8
D	II	0.20	10	2.2	42
E	II	0.18	9	3.9	40.4
F	II	0.18	8	2	46.1

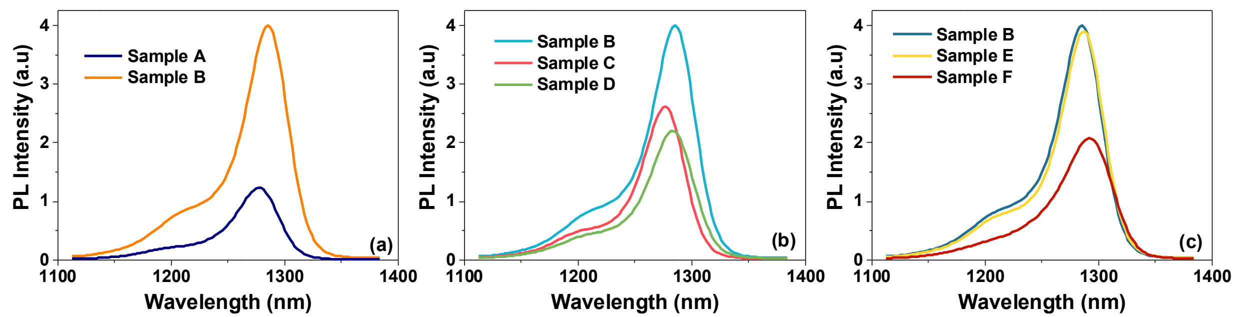

Fig.3 PL spectra of (a) sample A to B (b) sample B, C and D (c) sample B, E and F.

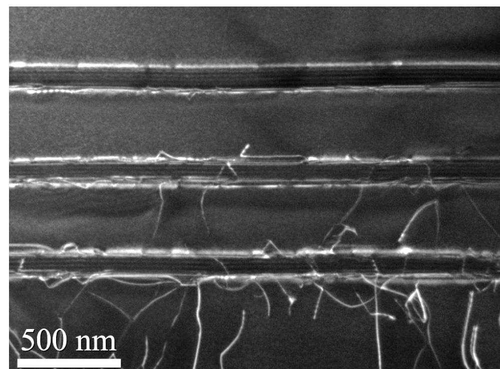

Fig 4. Bright-field TEM cross-section image of InGaAs/GaAs DFLs grow on a Si substrate.

Downloaded From: https://www.spiedigitallibrary.org/conference-proceedings-of-spie on 9/1/2017 Terms of Use: https://spiedigitallibrary.spie.org/ss/TermsOfUse.aspx

3. LONG LIFE ELECTRICALLY PUMPED III-V QUANTUM DOTS LASER

3.1 Growth and fabrication of Laser structure

Si-based QD laser devices have been further investigated by exploiting the results of optimization of DFLs in Section 2. A 4° off-cut phosphorus-doped Si (100) substrate is used to annihilate APDs. In order to improve the epitaxy growth between the interface of Si and III-V compounds, an AlAs nucleation layer with 6 nm thickness (Fig. 5a) was grown first at a low growth temperature of 350 °C. After that, a 1 μm thick GaAs buffer layer was grown using a three-step growth technique at 350, 450 and 590 °C for 30, 170 and 800 nm, respectively. Fig.5 (b) is a TEM image of the GaAs buffer and DFLs. Most of dislocations are well confined in the first 200 nm buffer layer (position 1), which is attributed to the AlAs nucleation layer and good crystal of GaAs buffer layer using the three step growth method. Five sets of optimized $In_{0.18}Ga_{0.82}As$/GaAs SLSs DFLs are grown with the purpose of reducing the high TD density and stopping propagation of TDs into the active region. In-situ thermal annealing of SLSs was also performed in the MBE reactor in order to further improve the efficacy of DFLs, by increasing the motion of defects and thereby raising the probability of annihilation between the defects. As shown in Fig.5 (c), the TD density before the first set of SLSs (position 1) is greater than 1×10^{9} cm^{-2}. It has been significantly reduced to the order of 1×10^{5} cm^{-2} after five sets of SLSs. Five layers of InAs/GaAs DWELL structures with good QD uniformity and a dot density of around 3×10^{10} cm^{-2} were formed as active region, where a PL emission at 1,300 nm was obtained (Fig. 6d). Each layer of DWELL comprised a 3ML InAs QD in the middle of 2 nm $In_{0.15}Ga_{0.85}As$ and 6 nm $In_{0.15}Ga_{0.85}As$, and was separated by 50 nm GaAs spacer layer. The whole DWELL structures were sandwiched between 1.4 μm $Al_{0.4}Ga_{0.6}As$ p-doped and n-doped cladding layers. Finally, a 300 nm highly p-doped GaAs was grown as the contacting layer.

This lasers were fabricated as 50 μm wide stripe broad-area lasers by using standard lithography and wet chemical etching techniques (Fig. 6). The ridge was etched to about 100 nm above the active region in order to give improved carrier confinement. Ti/Pt/Au and Ni/GeAu/Ni/Au were deposited on the p^{+}- GaAs contact layer and exposed n^{+}- GaAs buffer layer to form the p- and n- contacts. The lasers were cleaved to mirror-like facets and no facet coating was applied, as shown in Fig. 6.

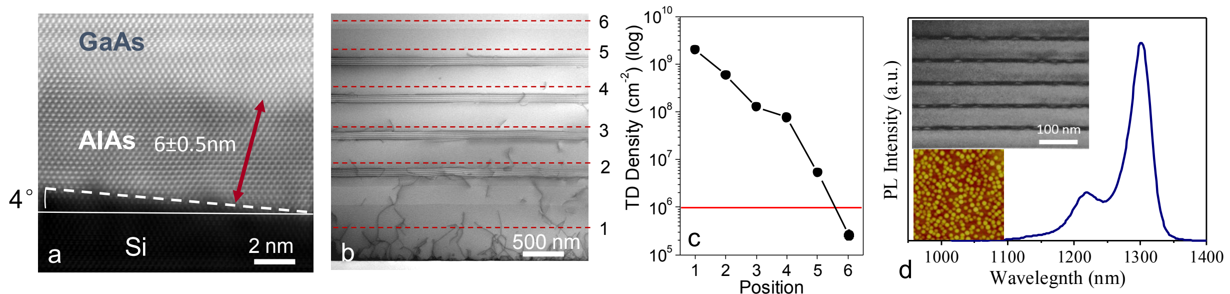

Figure 5. (a) 6 nm AlAs nuclear layer between 4° offcut Si substrate and GaAs buffer layer (b) cross-section TEM image of DFLs with 6 positions (c) Dislocation density corresponding to 6 positions (d) PL spectrum of QD active region grown on Si. Inset: Bright-field TEM image of DWELL (top left), AFM image of uncapped QDs layer (bottom left)

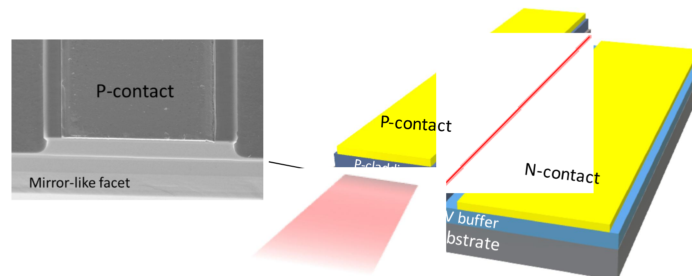

Figure 6. Schematic of InAs/GaAs QDs broad area Laser on Si substrate with mirror-like facet.

Downloaded From: https://www.spiedigitallibrary.org/conference-proceedings-of-spie on 9/1/2017 Terms of Use: https://spiedigitallibrary.spie.org/ss/TermsOfUse.aspx

3.2 Results and Discussion

Fig. 7 (a) shows the light-current-voltage (LIV) characteristic measurement of the III-V QD laser on Si under c.w. operation at room temperature. This laser achieved the extremely low threshold current density of 62.5 A cm^{-2} and over 100 mW output power when the injection current density is 650 A cm^{-2}. Temperature dependence measurements were also carried out. The lasers can lase up to 75 °C heat-sink temperature in the c.w. mode (Fig.7 b) and up to 120 °C in pulsed mode. The characteristic temperature T_0 has been calculated under pulsed operation as 51 K ranging from 20 to 60 °C and 35 K from 70 to 120 °C. The temperature sensitivity can be improved by using p-doped QD and mounting the laser on a high thermal conductivity heat-sink in future work.

The emission spectra for this III-V QD on Si laser variation at different current densities were determined under c.w. operation at room temperature in Fig.7 (c). When the current density was 50 A cm^{-2}, spontaneous emission was observed with broad FWHM of 38 nm at 1316 nm wavelength. As the injection current density was increased to 62.5 A cm^{-2}, a typical lasing emission was observed with sharply increased intensity and narrowed FWHM (2.4 nm). At higher current densities, multi-mode lasing behaviour, characteristic of a broad area laser, was observed in the emission spectra. In addition, we implemented a lifetime study on this Si-based InAs/GaAs QD laser. The ageing test was undertaken at a constant c.w. drive current of 210 mA with the output power monitored, at a fixed temperature of 26 °C. The ageing results are depicted in Fig. 7d where a 29.7% drop in power over the first 3,100 h continuous operation is observed. By fitting the threshold current trend with a sub-linear model an extrapolated lifetime of over 100,158 h was determined.

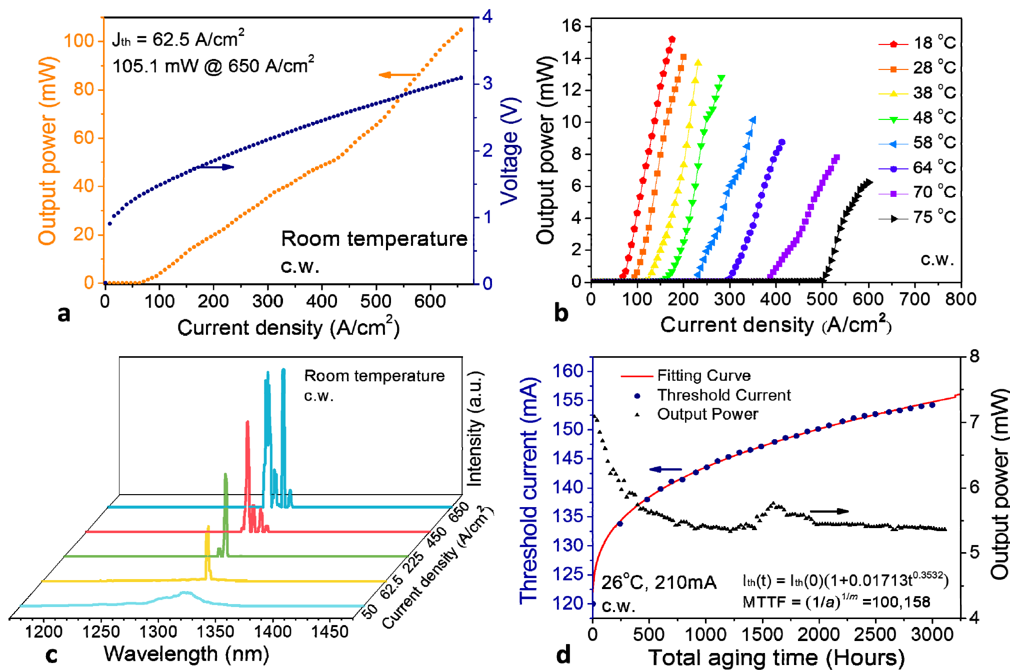

Figure 7. (a) Light-current-voltage (LIV) measurement of InAs/GaAs QDs laser on Si under c.w. operation at room temperature. (b) Light-current (L-I) characteristic of lasers at different temperatures under c.w. operation. (c) Emission spectra of Si-based lasers with different current densities under c.w. operstion. (d) Plots of threshold current and output power against total ageing time (hours) at 26 °C with 210 mA c.w. drive current.

Downloaded From: https://www.spiedigitallibrary.org/conference-proceedings-of-spie on 9/1/2017 Terms of Use: https://spiedigitallibrary.spie.org/ss/TermsOfUse.aspx

4. CONCLUSION

In this paper, we have firstly investigated the optimization of InGaAs/GaAs SLSs DFLs with three variations: i) the growth condition of GaAs spacer layers; ii) the indium composition of InGaAs SLSs; and iii) the thickness of GaAs in SLSs. Comparison and analysis for each sample was carried out in order to achieve maximum efficacy of DFLs. This effort combined with the use of an AlAs nucleation layer, three step GaAs buffer layer growth and using QDs in the active region contributes to a remarkable result of an electrically-pumped III-V QD laser directly grown on Si substrate. Current density of 62.5 A cm^{-2} and over 105 mw output power under c.w. operation were achieved from these lasers, which can lase up to 120°C under pulsed operation. Finally, an extrapolated lifetime of over 100,158 h lifetime provides a major step to delivering commercial III-V QD lasers on Si substrates.

REFERENCE

[1] Liang, D. and Bowers, J. E., "Recent progress in lasers on Silicon," Nat. Photonics 4(8), 511–517 (2010).

[2] G. T. Reed, G. Mashanovich, F. Y. Gardes, and D. J. Thomson, "Silicon optical modulators," Nat. Photonics 4(8), 518–526 (2010).

[3] Michel, J., Liu, J., Kimerling, L. C. High-performance Ge-on-Si photodetector. Nat. Photonics 4, 527−534 (2010).

[4] Chen, R., Tran, T.-T., Ng, K.W., Ko, W.S., Chang, L.C., Sedgwick, F. G. and Chang-Hasnain, C.: 'Nanolasers grown on silicon', Nat. Photonics 5(3), 170–175 (2011)

[5] Sugawara, M., Usami, M., "Quantum dot device handing the heat," Nat. Photonics, 3, 30-31 (2009).

[6] Liu, H., Wang, T., Jiang, Q., Hogg, R., Tutu, F., Pozzi, F. and Seeds, A., "Long-wavelength InAs/GaAs quantum-dot laser diode monolithically grown on Ge substrate," Nat. Photon., 5, 416–419(2011).

[7] Wang, T., Liu, H., Lee, A., Pozzi, F., and Seeds, A., "1.3-μm InAs/GaAs quantum-dot lasers monolithically grown on Si substrates," Opt. Express 19(12), 11381–11386 (2011).

[8] Lee, A., Jiang, Q., Tang, M., Seed, A. and Liu, H., "Continuous-wave InAs/GaAs quantum-dot laser diodes monolithically grown on Si substrate with low threshold current densities," Opt. Express, 20, 22181–22187 (2012).

[9] Lee, A.D., Jiang, Q., Tang, M., Zhang, Y., Seeds, A.J. and Liu, H, "InAs/GaAs quantum-dot lasers monolithically grown on Si, Ge, and Ge-on-Si substrates," IEEE J. Sel. Top. Quantum Electron., 19, 1901107–1–1901107–7 (2013).

[10] Liu, A.Y., Zhang, C., Norman, J., Snyder, A., Lubyshev, D., Fastenau, J.M., Liu, A.W., Gossard, A.C. and Bowers, J.E., "High performance continuous wave 1.3 μm quantum dot lasers on silicon," Appl. Phys. Lett., 104, 041104–1–041104–4 (2014).

[11] Liu, H., Childs, D., Badcock, T., Groom, K., Sellers, I., Hopkinson, M., Hogg, R., Robbins, D., Mowbray, D., and Skolnick, M., "High-performance three-layer 1.3-μm InAs-GaAs quantum-dot lasers with very low continuous-wave room-temperature threshold currents," IEEE Photon. Technol. Lett. 17, 1139-1141 (2005).

[12] Liu, A. Y., Herrick, R. W., Ueda, O., petroff, P. M., Gossard, A. C. and Bowers, J. E., "Reliability of InAs/GaAs Quantum Dot Lasers Epitaxially Grown on Silicon," IEEE J. Select. Topics Quantum Electron, 21(6), 1900708 (2015).

[13] Chang. H. H. et al., "1310 nm silicon evanescent laser," Opt. Exp., vol. 15, no. 18, pp. 11466-11471 (2007).

[14] Tang, M., Chen, S., Wu, J., Jiang, Q., Dorogan, V.G., Benamara, M., Mazur, Y.I., Salamo, G.J., Seeds, A. and Liu, H., "1.3-μm InAs/GaAs quantum-dot lasers monolithically grown on Si substrates using InAlAs/GaAs dislocation filter layers," Opt. Express, 22, 11528–11535 (2014).

[15] Chen, S., Tang, M., Jiang, Q., Wu, J., Dorogan, V.G., Benamara, M., Mazur, Y.I., Salamo, G.J., Seeds, A. and Liu, H. "1.3-μm InAs/GaAs quantum-dot laser monolithically grown on Si Substrates operating over 100°C," Electron. Lett., 50, 1467–1468 (2014).

Downloaded From: https://www.spiedigitallibrary.org/conference-proceedings-of-spie on 9/1/2017 Terms of Use: https://spiedigitallibrary.spie.org/ss/TermsOfUse.aspx

[16] Tang, M., Wu, J., Chen, S., Jiang Q., Seeds, A., Liu, H., Dorogan, V.G., Benamara, M., Mazur, Y.I., Salamo, G., "Optimisation of the dislocation filter layers in 1.3-μm InAs/GaAs quantum-dot lasers monolithically grown on Si substrates," J. IET Optoelectronics, 61-64 (2015).
[17] Tang, M., Chen, S., Wu, J., Kennedy, K., Jurczak, P., Liao, M., Beanland, R., Seeds, A. and Liu. H., "Optimizations of defect filter layers for 1.3- μm InAs-GaAs quantum-dot lasers monolithically grown on si substrates," IEEE JSTQE, vol. 22, no.6, 2551941(2016).
[18] Chen, S., Li, W., Wu, J., Jiang, Q., Tang, M., Shutts, S., Elliott, S.N., Sobiesierski, A., Seeds, A.J., Ross, I., Smowton, P.M., and Liu, H., "Electrically pumped continuous-wave III-V quantum dot lasers on silicon," Nature Photonics 10, 307–311 (2016)

Downloaded From: https://www.spiedigitallibrary.org/conference-proceedings-of-spie on 9/1/2017 Terms of Use: https://spiedigitallibrary.spie.org/ss/TermsOfUse.aspx